Roux-en-Y reconstruction alleviates radical gastrectomy-induced colitis via down-regulation of the butyrate/NLRP3 signaling pathway

Yizhou Yao,[a,c] Shishuo Sun,[b,c] Jinrong Gu,[a] Haishun Ni,[a] Kaiqiang Zhong,[a] Qixuan Xu,[a] Diyuan Zhou,[a] Xuchao Wang,[a] Ling Gao,[a] and Xinguo Zhu[a,*]

[a]Department of General Surgery, The First Affiliated Hospital of Soochow University, Suzhou, Jiangsu, China
[b]Cancer Institute, The First Clinical Medical College, Xuzhou Medical University, Xuzhou, Jiangsu, China

Summary

Background Different methods for digestive tract reconstruction have a complex impact on the nutritional status of gastric cancer (GC) patients after radical gastrectomy. Previous studies reported that Roux-en-Y (R-Y) reconstruction resulted in obvious weight reduction and improvement in type 2 diabetes in obese patients. We investigated the relationship between R-Y reconstruction, gut microbiota, and the NLRP3 inflammasome in GC patients with poor basic nutrition.

Methods Changes in the gut microbiota after radical gastrectomy accomplished by different methods of digestive tract reconstruction were investigated via fecal microbiota transplantation. The underlying mechanisms were also explored by analyzing the role of the microbiota, butyrate, and the NLRP3 inflammasome in the colon tissues of colitis model mice and GC patients after radical gastrectomy.

Findings R-Y reconstruction effectively relieved intestinal inflammation and facilitated nutrient absorption. 16S rRNA analysis revealed that gavage transplantation with the fecal microbiota of R-Y reconstruction patients could reverse dysbacteriosis triggered by radical gastrectomy and elevate the relative abundance of some short-chain fatty acid (SCFA)-producing bacteria. Subsequently, butyrate negatively regulated the NLRP3-mediated inflammatory signaling pathway to inhibit the activation of macrophages and the secretion of pro-inflammatory mediators such as caspase-1 and interleukin (IL)-1β, decreasing the level of intestinal inflammation and promoting nutrient absorption.

Interpretation R-Y reconstruction induced colonization with SCFA-producing bacteria to alleviate radical gastrectomy-induced colitis by down-regulating the NLRP3 signaling pathway. This can be a new strategy and theoretical basis for the management of the postoperative nutritional status of GC patients.

Funding This work was supported by the National Nature Science Foundation of China (81974375), the BoXi cultivation program (BXQN202130), and the Project of Youth Foundation in Science and Education of the Department of Public Health of Suzhou (KJXW2018001).

Keywords: Gut microbiota; Radical gastrectomy; Roux-en-Y reconstruction; NLRP3 inflammasome; Butyrate

Introduction

Gastric cancer (GC) is a malignancy of the digestive tract that occurs with high incidence, accounting for approximately 10% of all cancer-related deaths worldwide.[1,2] Digestive tract reconstruction is one of the main factors affecting the nutritional status and quality of life of patients after gastrectomy. However, there is rare consensus among studies on the impact of different digestive tract reconstruction methods.[3–5] As an important factor affecting the survival prognosis and quality of life of the patients, the effects of digestive tract reconstruction on the homeostasis of the intestinal microenvironment and intestinal nutrient absorption represent complex biological processes.

*Corresponding author.
E-mail address: xgzhu@suda.edu.cn (X. Zhu).
[c]Equally contribution.

Research in context

Evidence before this study
Compared to B-I and B-II, R-Y reconstruction preserves the normal anatomical structure and can prevent bile reflux. Changes in the structure of the digestive tract are closely related to alterations in gut microbiota abundance. The gut microbiota regulates short-chain fatty acid metabolism and affects intestinal inflammation levels. However, for patients with poor basic nutritional status, the effect of the selected digestive tract reconstruction method on nutrient absorption after radical gastrectomy is not clear.

Added value of this study
Here, we reported that R-Y reconstruction alleviated intestinal inflammation by increasing the abundance of butyrate-producing bacteria, inhibiting the NLRP3 inflammasome by butyrate production, and ultimately maintaining postoperative nutrient absorption in patients with poor basic

nutrition. R-Y reconstruction could be a qualified selection that regulates gut microbiota to exert anti-inflammatory effects and provides the microbial metabolite butyrate for GC patients with poor basic nutrition.

Implications of all the available evidence
Our results not only demonstrated that R-Y reconstruction affected the composition of intestinal microbiota and increased the butyrate content, but they also emphasize that butyrate inhibited NLRP3-related intestinal inflammation, maintained intestinal homeostasis and the integrity of the intestinal wall structure, and facilitated nutrition absorption. Given that gastric cancers are usually diagnosed at an advanced stage in patients with poor basic nutrition, our results provide a qualified reconstruction method to improve the clinical management and outcomes of the patients.

The Billroth-I (B-I), Billroth-II (B-II), and Roux-en-Y (R-Y) reconstruction methods are considered to be reliable choices for digestive tract reconstruction after radical treatment for distal GC. Although a few studies have compared the effects of various digestive tract reconstruction methods on the clinical indicators of patients after surgery, the results varied greatly.[3,5,6] Different reconstruction methods lead to differences in the locations where food and secreted bile contact the intestinal mucosa. Anatomical changes caused by different gastrointestinal reconstruction methods may have different effects on intestinal hormone levels.[7–9] In patients with GC accompanied by type 2 diabetes, related clinical indicators were improved in 27.8% of the patients who received R-Y reconstruction and 5.9% of those who received B-II reconstruction, and their body mass index (BMI) values were correspondingly reduced, although the improvement rate was lower than that of obese patients undergoing gastric reduction surgery as described in previous studies.[9,10]

Previous studies have focused on the role of digestive tract reconstruction in weight reduction and improvements in type 2 diabetes in obese patients with high BMIs.[11,12] However, the preoperative basic nutritional status is poor in some patients with advanced GC. Few studies have focused on the nutritional status of patients undergoing digestive tract reconstruction after radical gastrectomy, and the mechanism underlying the postoperative recovery stage remains to be elucidated. NLRP3, in the NOD-like receptor family member, is a cytoplasmic protein complex which facilitates the secretion of inflammatory cytokines IL-1β and IL-18.[13] Recent evidence demonstrated that nutrient absorption disorder was closely correlated with NLRP3 inflammasome activation in the gut.[14] The NLRP3 inflammasome is well-characterized by its ability to control the activation of caspase-1.[15,16] It is mainly composed of a sensor protein, pro-inflammatory caspase-1, and adaptor protein apoptosis-related spot-like protein.[17,18] It is also responsible for proteolytic maturation and the secretion of pro-inflammatory cytokines IL-1β and IL-18.[19,20] As a vital innate immune sensor, NLRP3 inflammasome stimulation was responsible for wear particles inducing an immune response in human macrophages.[21] Thus, the downregulation of the NLRP3 inflammasome by selected digestive tract reconstruction methods may represent a potential treatment for improving the nutritional status of GC patients after surgery.

In this study, we investigated whether R-Y reconstruction could reprogram the gut microbiota in patients eating a normal diet and increase the concentration of short-chain fatty acids (SCFAs). Then, we examined whether R-Y reconstruction inhibited the NLRP3-mediated inflammatory signaling pathway by promoting butyrate secretion. Finally, we explored its effects on alleviating intestinal inflammation and blocking the process of colitis induced by radical gastrectomy. The results may provide a theoretical basis for selecting the digestive tract reconstruction method for GC patients with different nutritional status.

Methods
Study population
All patients included in this study underwent laparoscopic distal gastrectomy at the First Affiliated Hospital of Soochow University between January 2016 and February 2019. Patients with radical distal gastrectomy underwent one of the three different methods for digestive tract reconstruction. (1) B-I reconstruction:

The duodenum and remnant stomach were anastomosed via hand-sewing or a circular stapler. (2) B-II reconstruction: A small opening was made in the jejunum, 15 cm from the Treitz ligament on the anti-mesenteric margin and the posterior gastric wall. A linear stapler was inserted into the opening to perform gastrojejunostomy. Then, the common opening was closed using absorbable barbed wire. (3) R-Y reconstruction: The jejunum was cut off at a distance of 15 cm from the Treitz ligament, the anastomosis coincided with the remnant and the distal jejunum, and the proximal and distal ends of the jejunum were anastomosed at a distance of approximately 40 cm below the gastro-jejunal anastomotic site.

The following inclusion criteria were applied: (1) pathologically confirmed gastric cancer, (2) complete preoperative CT imaging data and laboratory data, (3) TNM stage II–III, and (4) preoperative gastroscopy and CT confirmed that the tumor was located in the middle and lower part of the stomach, which was estimated to meet the requirements of a distal radical resection margin. The exclusion criteria were: (1) preoperative chemotherapy or radiotherapy, (2) lack of relevant clinical indicators, (3) any other malignant tumors or neurodegenerative disorders, (4) history of gastrointestinal surgery, (5) history of inflammatory bowel disease, and (6) patients with serious heart or lung disease or other serious organ dysfunction. Two experienced surgeons participated independently in collecting, recording, and reviewing the clinical characteristics.

Pre-experimental findings suggested that mean BMI change rate in R-Y, B-I, and B-II reconstructions from baseline to one year after surgery was −0.040, −0.100, and −0.100, respectively, assuming a standard deviation of 0.07. The difference test was used to estimate the sample size with 90% test power and a 5% significance level. Accounting for a 20% drop-out rate and 1:1:1 allocation ratio, the total number of patients required per group was 34 (approximately 102 in total). An approximately similar number of patients who met the inclusion criteria were continuously included in this study, and stool samples were collected based on the estimated sample size.

Preoperative stool samples were collected from the patients, and the method of digestive tract reconstruction after radical gastrectomy was recorded. Stool samples were also collected from the patients preoperatively and one year after surgery. When we collected the patient's feces, the patient laid a clean paper on a disposable bedpan and defecated on it. A sterile spoon or a sterile cotton swab was used to dig out the internal part of the stool that did not contact the air or the paper. A portion the size of a soybean was removed and put into a sterile sample tube, an information label was applied and the sample was stored in liquid nitrogen. We excluded the patients' condition of constipation or diarrhea to avoid affecting the results. One hundred and six patients were enrolled in this study and all of the patients provided written informed consent. The related information on the patients is shown in Supplementary Table S1–S3.

Establishment of the colitis mouse model

Specific pathogen-free-grade male C57BL/6 mice (aged 4–6 weeks, Shanghai Institutes for Biological Sciences) were fed sterile food and water and maintained in sterile isolators. The mice were randomly assigned to each group. To meet the 3R principle and the calculation of sample size, the sample size calculation was performed after doing a pilot study with 6 C57BL/6 mice per group. Based on the outcome of this pilot study, we calculated number of mice per group at confidence interval of 95% and power of 90% to get a P-value less than 0.05.[22–24] The predicted number of mice to be kept in each group was calculated, n = 6. Ciprofloxacin (0.2 g/L) and metronidazole (1 g/L) were added to drinking water for intestinal pretreatment for 2 weeks. Then, the mice were given drinking water containing 2.5% dextran sulfate sodium (DSS) to construct the enteritis model.

To generate DSS-induced colitis model mice, the mice were fed 2.5% DSS for 5 consecutive days and then changed to normal water for another 5 days. Body weight, stool consistency (0, normal; 2, loose feces; 4, diarrhea), and hematochezia (0, occult blood negative; 2, occult blood positive; 4, gross bloody stool) were daily measured and recorded as previously described.[25] Mice were euthanized by cervical dislocation on day 10, and the colon length and spleen weight were measured. Tissue samples were frozen in liquid nitrogen or fixed in 10% formalin for further analysis. The entire colon was stained with hematoxylin and eosin (H&E) and Alcian blue. Colon inflammation, area, hyperplasia, and dysplasia of the mucosa and submucosa were observed by H&E staining. Acidic mucus-containing goblet cells were identified by Alcian blue staining. The results were evaluated by two authors who were blinded to each other.[19]

Fecal microbiota transplantation (FMT)

Fecal samples (200 mg) obtained from patients one year after B-I, B-II, and R-Y reconstruction were mixed thoroughly with 5 mL of phosphate-buffered saline (PBS) under anaerobic conditions. After centrifugation at 600 rpm for 3 min, the supernatant was collected and 200 μL was used to transplant fecal bacteria into the mice by gavage every day.

Immunohistochemical and immunofluorescence staining

The colon contents were emptied from the proximal to the distal end and the intestine was cut lengthwise and soaked in 10% formalin for 24 h. The tissues were

embedded in paraffin and 5-µm sections were cut for immunohistochemical staining as previously described.[26] They were also incubated with indicated primary antibodies followed by Alexa Fluor 488-conjugated secondary antibodies for immunofluorescence staining.[27] The slides were then washed 3 times and stained with DAPI (4′,6-diamidino-2-phenylindole). The images were taken with a Nikon ECLIPSE Ni microscope equipped with a color camera and were processed by ImageJ software.[28] Five randomly selected regions were analyzed per sample.

Fatty acid detection by GC–MS

Stool samples from mice were collected and analyzed SCFA levels. Fecal samples from the ileocecal region of mice were collected during the same time period and stored in liquid nitrogen until SCFA analysis was performed. A standard curve of fatty acid methyl esters (1000 g/mL) was prepared in n-hexane at concentrations of 1, 5, 10, 25, 50, 100, 250, 500 and 1000 mL. Each sample (50 mg) was mixed with 2 mL of a 1% sulfuric acid-methanol solution, mixed thoroughly for 1 min, and placed in a water bath at 80 °C. After 30 min of methylation, 1 mL of n-hexane was added for extraction, and the sample was washed with 5 mL of pure water. The supernatant (500 µL) was added to 100 mg of anhydrous sodium sulfate to remove excess water and internal label was added to the supernatant for testing. After gas chromatography–mass spectroscopy (GC–MS) detection, the samples were quantitatively analyzed by referring to the standard curve.[26,29]

16S rRNA sequencing

The 16S rRNA sequencing community map was identified by the Illumina HiSeq sequencing V4 region (insertion size of 300 bp; read length of 250 bp). Sequences were reaggregated with 97% sequence consistency, and chimeras were removed by UPARSE. For each representative sequence, the GreenGene database was used to label its classification information. The changes in bacterial abundance were analyzed, and the bacteria with great differences were selected as candidates.

Detection of macrophage cell activation

The RAW264.7 macrophage cell line (from the American Type Culture Collection) was treated for 8 h with acetate, propionate, and butyrate (1 mM). The expression of PE-INOS (inducible nitric oxide synthase) was detected by flow cytometry to assess M1 macrophage polarization. RAW264.7 cells were also treated for 8 h with a combination of SCFAs (1 mM) and lipopolysaccharide (LPS, 100 ng/mL), and M1 polarization was investigated as previously described.[28] The cell lines used in this study were previously authenticated.

Protein extraction and Western blot analysis

Total proteins were separated by sodium dodecyl sulfate-polyacrylamide gel electrophoresis (SDS-PAGE) and transferred onto polyvinylidene fluoride (PVDF) membranes, which were blocked with 5% non-fat milk and incubated sequentially with the indicated primary antibodies and horseradish peroxidase-conjugated secondary antibodies. The proteins were visualized by chemiluminescence and signals were quantified by ImageJ software. The antibodies used in this study are listed in Supplementary Table S4.

Ethics statement

This study was conducted in accordance with the standards of the Declaration of Helsinki and current ethical guidelines and was approved by the Institutional Ethics Committee of the First Affiliated Hospital of Soochow University (reference number: 2020086). All participants provided written informed consent to participate in the study. All animal experimental procedures were approved by the Animal Ethics Committee of the First Affiliated Hospital of Soochow University according to the ARRIVE guidelines 2.0 (reference number: 2021110).[30]

Statistical methods

All numerical data were verified by the assumption of normality using Shapro-Wilk test. Data normally distributed are presented as the mean ± SEM or SD of at least three independent experiments, while data not normally distributed are described by the median, and 25th and 75th percentiles. The student's t-test (unpaired, two-tailed), Mann–Whitney U test (unpaired, two-tailed), one-way analysis of variance (ANOVA), and the Kruskal–Wallis test were used to compare means between the groups. Bonferroni's correction was used to correct for multiple testing. Categorical data were analyzed by chi-squared or Fisher's exact tests.

Spearman's correlation analysis was used to examine the correlations between the prognostic nutritional index (PNI) value and the rate of change in BMIs. Principal coordinates analysis (PCoA) was used to perform the cluster analysis of patients with R-Y, B-I, and B-II digestive tract reconstructions, and PCoA subgroup analysis based on preoperative BMI values was performed. Permutational multivariate analysis of variance (PERMANOVA) was applied to analyze different nutritional statuses between the three groups.

Propensity score matching patients were categorized into three groups based on digestive tract reconstructions. Patients in groups were matched using the propensity score method. The propensity score for an individual was calculated according to demographics information. Shannon and Simpson alpha-diversity indexes were calculated to estimate microbial diversity

between the R-Y and control groups. Effect size estimation, tests of biological consistency, and class comparison were determined by linear discriminant analysis effect size (LEfSe) analysis. A *P*-value of <0.05 was considered statistically significant. Statistical analyses were performed using SPSS 25.0 software (SPSS Inc., Chicago, IL, USA), GraphPad Prism 8 (San Diego, CA, USA), and R programs (version 4.1.3, https://cran.r-project.org/web/packages.html).

Role of the funding source

The funder of the study had no role in the study design, data collection, data analysis, data interpretation, or writing of the report.

Results

R-Y reconstruction improves postoperative nutritional status in patients with poor basic nutrition

In total, 106 patients who underwent laparoscopic radical gastrectomy for distal GC were included in this study. These patients were comprised of 38 patients with B-I type gastrointestinal reconstruction, 37 patients with B-II type, and 31 patients with R-Y type (Supplementary Tables S1–S3). The imaging-related nutritional indicators skeletal muscle index (SMI), visceral fat index (VFI), and subcutaneous fat index (SFI) were tracked and analyzed (Fig. 1A). The results revealed an obvious reduction in BMI one year after surgery in all patients. There were no significant differences in nutritional indicators, such as BMI, SMI, VFI, and SFI, between the groups ($P > 0.05$, Fig. 1B). Similar to the effects in obese patients with a BMI greater than 35 in previous studies, R-Y reconstruction after radical gastrectomy had a significant effect on reducing weight and alleviating type 2 diabetes in obese GC patients.[9,10] Therefore, we analyzed the patients in each group with a preoperative BMI below the median value to further explore this phenomenon. Interestingly, and in contrast to previous studies, the BMI and SMI of patients with poor basic nutrition who underwent R-Y reconstruction were better than those of patients in the B-I and B-II groups one year after surgery ($P < 0.05$, Fig. 1C).

In addition, in the analysis of the clinical indicators one year after surgery, there were no significant differences in hemoglobin (Hb), low-density lipoprotein (LDL), lymphocyte count, the neutrophil-to-lymphocyte ratio (NLR), or total cholesterol (TC) levels between the groups in both the overall analysis and the subgroup analysis of patients with preoperative BMIs below the median ($P > 0.05$). In the overall analysis, albumin (ALB), high-density lipoprotein (HDL), and the PNI in the R-Y group were higher than those in the B-I group ($P < 0.05$), whereas there were no differences in these

indicators between the R-Y group and the B-II group ($P > 0.05$). In patients with preoperative BMIs below the median, the PNI in the R-Y group was also higher than that of the B-I group ($P < 0.05$), although there was no significant difference between the R-Y group and the B-II group ($P > 0.05$, Supplementary Figure S1A). This suggests that the nutrition-related indicators ALB and PNI were superior in patients in the R-Y group compared to those in the B-I group, although there was no significant difference between the indicators in the R-Y and B-II groups.

Cluster analysis of the R-Y, B-I, and B-II digestive tract reconstruction patients was performed according to the rates of changes in the BMI, SMI, VIF, and SFI before and one year after surgery. For all included patients, there were no significant differences in principal coordinates (PC)1 and the PC2 axis between each group ($P > 0.05$), and the PERMANOVA analysis showed no significant differences between the three groups ($P > 0.05$, Fig. 1D). However, in the subgroup analysis of patients with preoperative BMI values below the median, there was a significant difference between the R-Y group and the B-I and B-II groups in the PC1 axis ($P = 0.001$ and $P = 0.037$, respectively), and the PERMANOVA analysis showed a statistically significant difference between the three groups ($P = 0.012$, Fig. 1E). We performed further cluster analysis based on the age and sex of the patients and performed subgroup analysis based on preoperative BMI values. The subgroup analysis showed that in patients with preoperative BMI values below the median, there was a significant difference in the rate of change in the BMI between elderly and young patients ($P = 0.014$, Supplementary Figure S1B). However, when the patients were grouped according to sex, no significant differences were found in the overall analysis and the subgroup analysis of patients with BMI values below the median ($P > 0.05$, Supplementary Figure S1C).

PNI predicts surgical risk, postoperative complications, and long-term prognosis by reflecting the patient's nutritional and immune statuses. The PNI is used to assess the nutritional status of GC patients and predict surgical risks and postoperative complications. However, few studies have been conducted on the correlation between the PNI and the nutritional prognosis of patients with radical gastrectomy. In this study, the correlation between PNI index values before and one year after surgery and the rate of change in the BMI during this period were analyzed. Postoperative PNI was positively correlated with the rate of change in the BMI ($r^2 = 0.038$, $P = 0.044$, Fig. 1F). In the subgroup analysis of patients with preoperative BMI values below the median, the postoperative PNI value was positively correlated with the rate of change in the BMI ($r^2 = 0.088$, $P = 0.032$, Fig. 1G), whereas there was no correlation in the subgroup analysis of patients with BMIs equal to or greater than the median ($r^2 = 0.011$, $P = 0.441$, Fig. 1H).
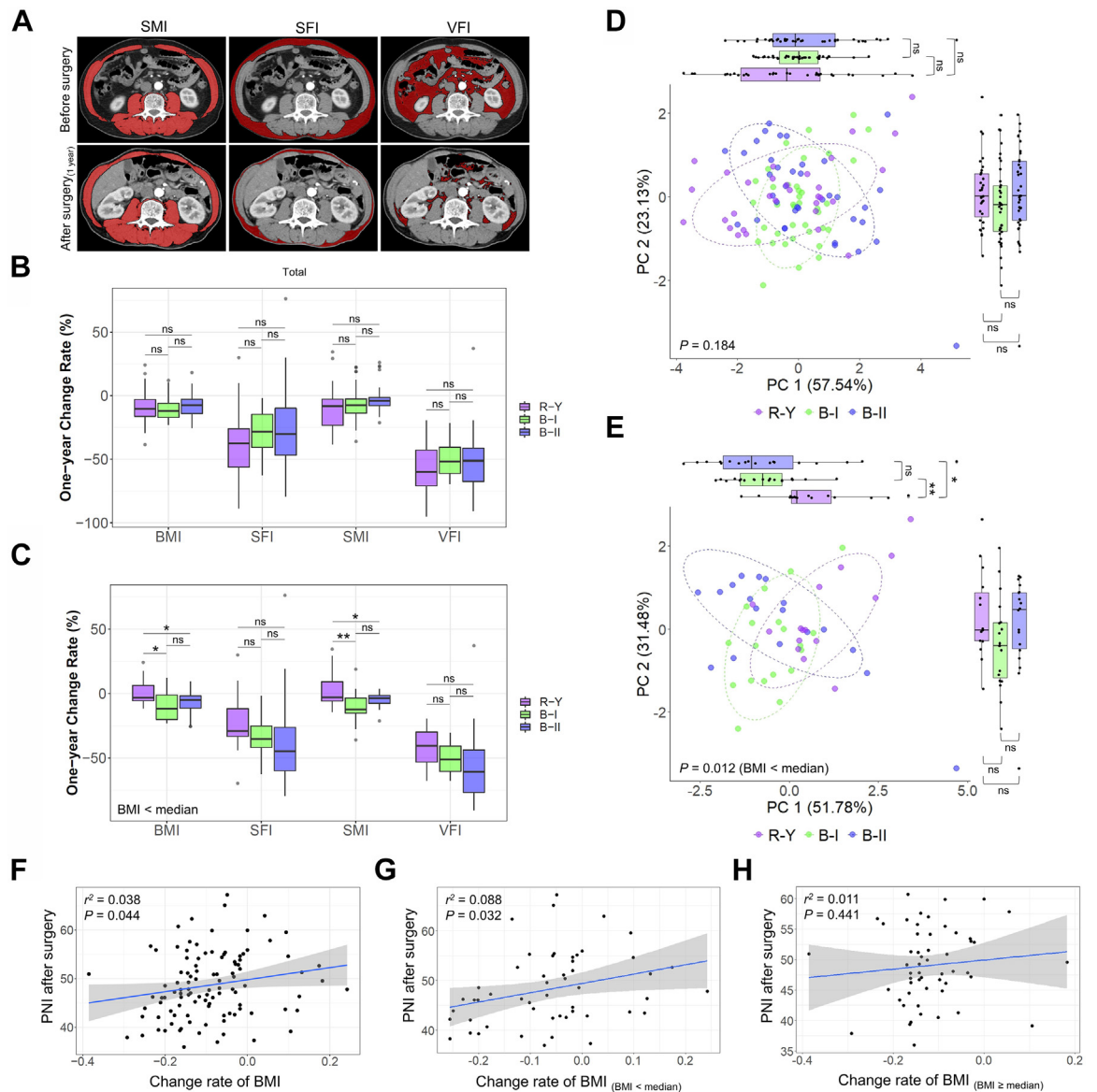
Fig. 1: Postoperative nutritional status of patients with different digestive tract reconstruction methods after radical gastrectomy. (A) Comparison of SMI, SFI, and VFI values preoperatively and one year after surgery. (B) Rates of changes in the SMI, SFI, VFI, and BMI before and one year after surgery in the B-I, B-II, and R-Y reconstruction groups. (C) Subgroup analysis of patients in each group with preoperative basic BMI values below the median. The rates of changes in the SMI, SFI, VFI, and BMI of patients in different digestive tract reconstruction groups before and one year after surgery. (D) Cluster analysis of the SMI, SFI, VFI, and BMI according to different digestive tract reconstruction methods. The axes represent the two most informative principal coordinates (PCs) of the PCoA analysis, with marginal boxplots describing the distribution in the different groups. The dots in different colors represent the variables analyzed. A pairwise test was used to compare PC1 or PC2 values between the groups, and P-values are shown beside the marginal boxplots. The results of the PERMANOVA to compare dissimilar indexes among the samples are shown in the lower-left corner of the figure. (E) Cluster analysis of preoperative BMIs below the median in each group and combined SMI, SFI, VFI, and BMI values according to different digestive tract reconstruction methods was performed. (F) Correlation between the PNI one year after surgery and the rate of change in BMI during this period. (G and H) Subgroup analysis of the correlation between the PNI one year after surgery and the rate of change in BMI during this period for preoperative BMI values below the median (G) and greater to or equal to the median (H).

Furthermore, the analysis of preoperative PNI values and the rate of change in BMIs indicated that there was no significant correlation between preoperative PNI values and the rate of change in BMIs in either the overall analysis or the subgroup analysis according to preoperative basic BMI values ($P > 0.05$, Supplementary Figure S1D–F).

Gut microbiota composition is altered by different digestive tract reconstruction techniques after radical gastrectomy

In the groups of patients who underwent radical gastrectomy with B-I, B-II, and R-Y digestive tract reconstructions in this study, six patients in each group were selected after propensity score matching (1:1:1) in GC patients with a preoperative BMI below the median according to the demographics before surgery. Fecal samples before surgery and one year after surgery were analyzed by 16S-rRNA sequencing. In the sequencing analysis of fecal samples collected one year after surgery, the Shannon and Simpson indexes of patients in the R-Y group were significantly higher than those in the B-I and B-II groups ($P < 0.05$, Fig. 2A and B). Bray–Curtis distance-based PCoA analysis indicated that the clustering of gut microbiota in the R-Y group was significantly different from that in the B-I and B-II groups (Fig. 2C). Compared to the control group, the relative abundances of *Bacteroides*, *Clostridium*, and *Ruminococcus* were significantly enriched in the R-Y group ($P < 0.05$, Fig. 2D). And *Bacteroides*, *Clostridium*, and *Ruminococcus* were closely associated with the secretion of SCFAs.[27,31,32]

Different from the alterations in gut microbiota after surgery, there was no significant difference in the Shannon and Simpson index values of fecal samples in the three groups before surgery ($P > 0.05$, Supplementary Figure S2A–B). Bray–Curtis distance-based PCoA analysis also suggested no obvious differences in the gut microbiota clustering of the three groups (Supplementary Figure S2C). The analysis of SCFAs-producing microbiota, including *Bifidobacterium*, *Bacteroides*, *Clostridium*, *Eubacterium*, and *Ruminococcus*, revealed no significant differences between the three groups before surgery (Supplementary Figure S2D). Gut microbiota alterations in the R-Y, B-I, and B-II groups indicated that compared to B-I and B-II reconstructions, R-Y reconstruction had the potential effect to elevate the abundance of SCFA-producing microbiota.

We also performed a LEfSe analysis of the fecal 16S rRNA gene sequencing data (Fig. 2E and F). In the fecal samples collected one year after surgery, the taxonomic cladogram obtained from this analysis highlighted significant enrichment in several taxa, mostly *Clostridium* and *Ruminococcus*, in the R-Y group compared to the B-I and B-II group ($P < 0.05$, Fig. 2F).

Colonization with microbiota from R-Y reconstruction inhibits the development of colitis in mice

Based on the above analysis of clinical data, R-Y reconstruction was beneficial to maintaining postoperative nutrition-related indicators in GC patients with poor basic nutritional status. R-Y reconstruction maintains the physiological structure of the digestive tract, which may maintain the homeostasis of the gut microbiota and the intestinal microenvironment.[33,34] Hence, we hypothesized that gastrointestinal reconstruction induces alterations in the gut microbiota to regulate intestinal inflammation and absorption functions. To determine the role of the microbiota in GC patients with R-Y reconstruction, we investigated the effect of FMT in mice and found that R-Y FMT effectively maintained the nutritional status of mice and reversed weight deteriorations caused by DSS ($P < 0.001$, Fig. 3A).

Intestinal inflammation activity was then assessed based on stool consistency, gross rectal bleeding, colon length, and spleen weight. As shown in Fig. 3B–F, compared to the DSS control group, neither B-I FMT nor B-II FMT mice showed obvious differences in intestinal inflammation ($P > 0.05$). R-Y FMT decreased the inflammation caused by DSS ($P < 0.05$). Then, H&E staining was performed on the entire colon of mice to evaluate the intestinal gland structure, and Alcian blue staining was performed to assess the morphology of the goblet cells. The mice were histologically graded according to the staining results (Fig. 3G). Compared to the mice in the other groups, mice in the R-Y group had lower histological scores, indicating lower intestinal inflammation, better intestinal mucosal glandular structure synthesis, less immune cell infiltration, and a reduced range of influences (Fig. 3H). Finally, the effect of R-Y FMT on intestinal inflammation was further evaluated by continuous feeding with 3.5% DSS.[25] As shown in Fig. 3I, R-Y FMT mice revealed a better survival time than mice in the control group ($P < 0.05$).

The above results indicated that FMT with the intestinal microbiota of GC patients with R-Y reconstruction could alleviate digestive tract inflammation in mice, and the effect in the R-Y FMT group was superior to that in the B-I and B-II FMT groups. M1/M2 polarization of macrophages plays an important role in intestinal inflammation.[28,35] To assess whether the effect of R-Y FMT was associated with M1/M2 macrophage polarization in mice colon tissue, we performed immunofluorescence staining for the colocalization of the macrophage marker F4/80 with the M1 macrophage marker NOS2 (Fig. 4A) or the M2 macrophage marker ARG1 (Fig. 4B). The results showed that F4/80$^+$NOS2$^+$ macrophages were markedly reduced in the R-Y FMT group, but the abundance of F4/80$^+$ARG1$^+$ macrophages was not obviously changed in the colon tissues.
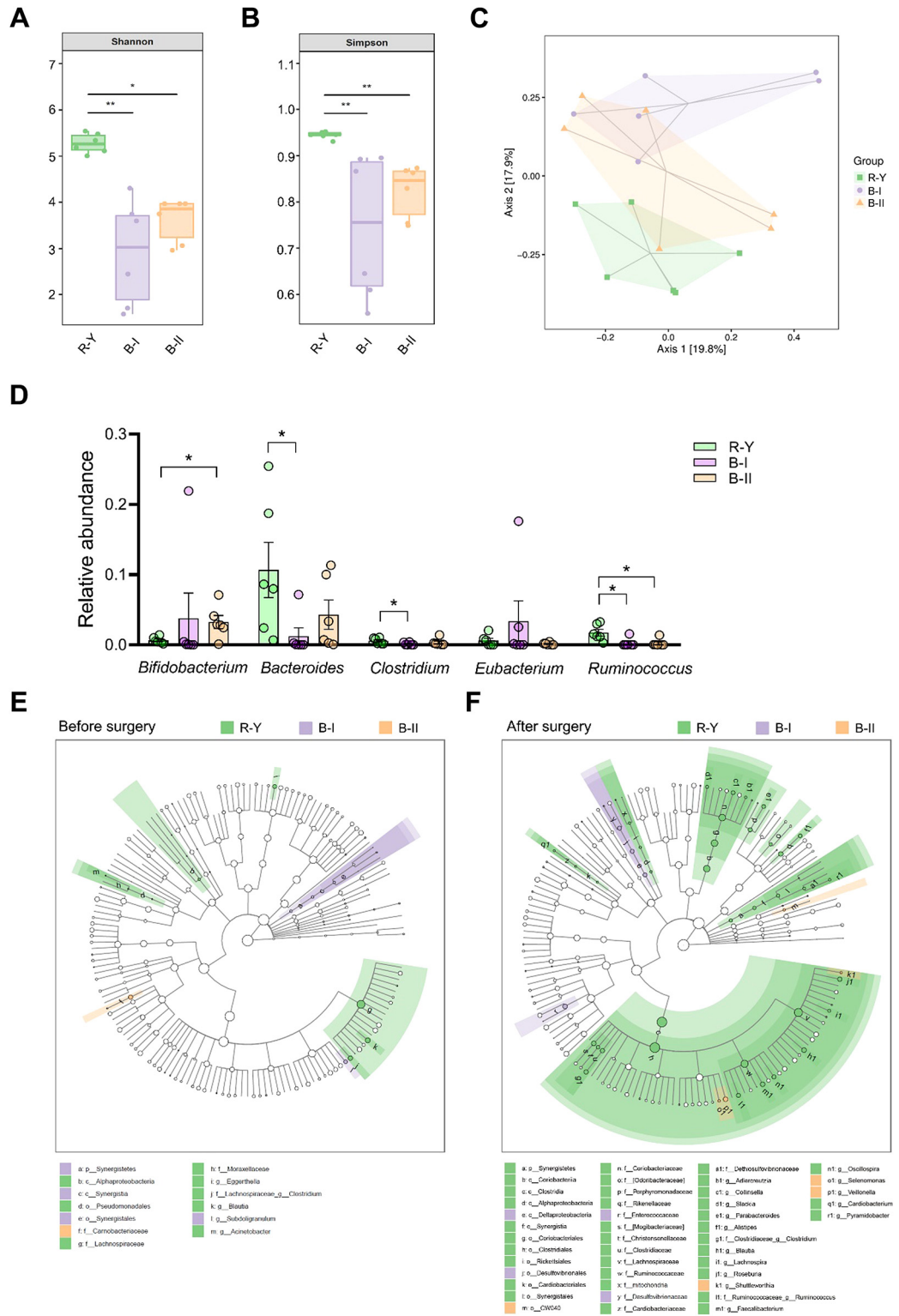
Fig. 2: Alterations in gut microbiota and different digestive tract reconstruction methods. (A and B) 16S-rRNA sequencing analysis of fecal samples from GC patients with R-Y, B-I, and B-II digestive tract reconstructions one year after surgery. Shannon (A) and Simpson (B) indexes were analyzed in each group; n = 6. (C) PCoA plot of the R-Y, B-I, and B-II groups based on Bray–Curtis distance; n = 6. (D) Relative abundance of SCFA-producing microbes in fecal samples; n = 6. (E and F) LEfSe analysis of gut microbiota alterations caused by gastrectomy and digestive tract reconstruction. Each group was analyzed before surgery (E) and after surgery (F); n = 6. Error bars represent the mean ± SEM. *P < 0.05.
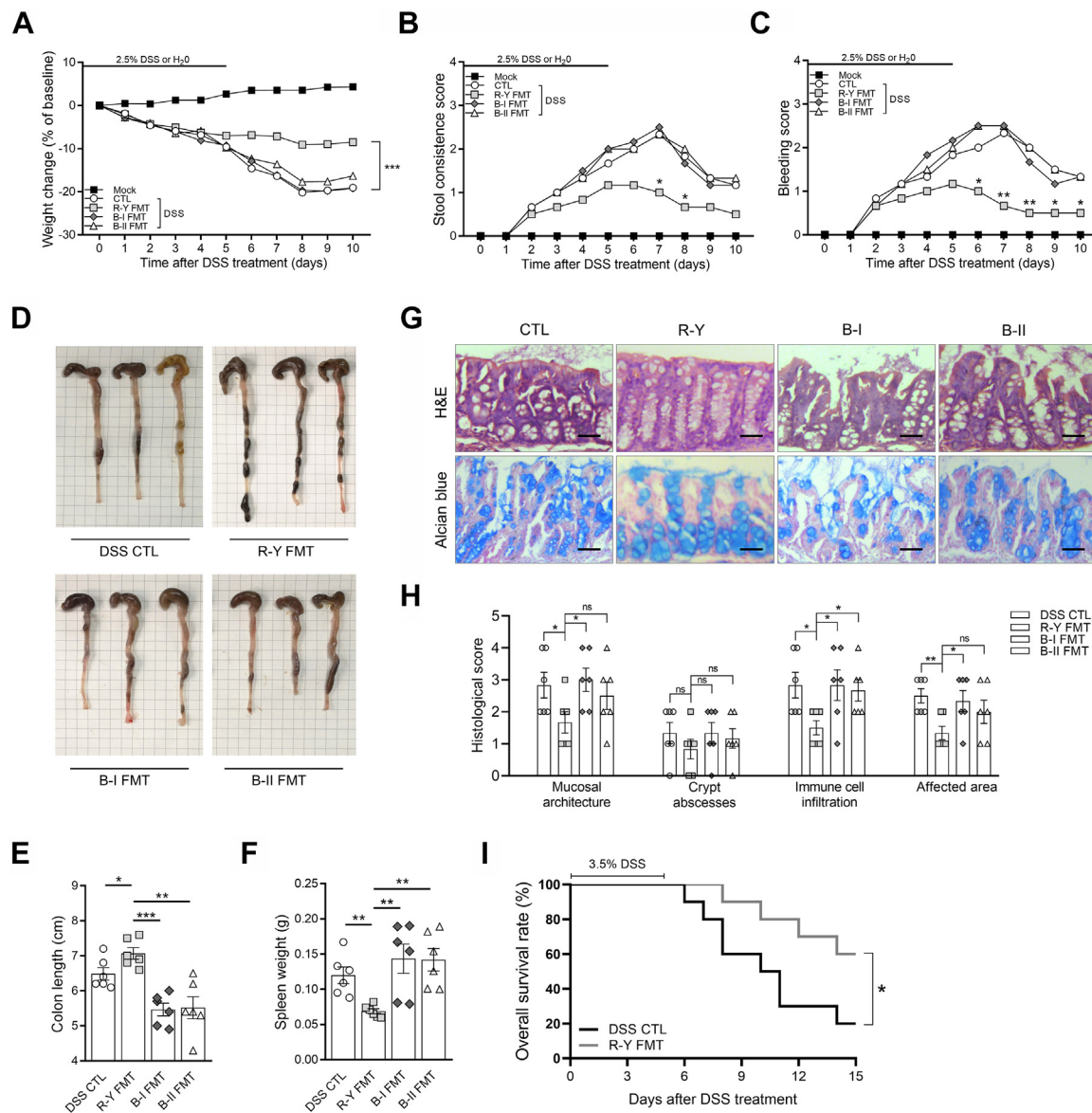
Fig. 3: Fecal transplantation with microbiota from patients with R-Y reconstruction relieves inflammation-driven colitis. (A–C) Weight change, stool consistency, and rectal bleeding score in mock, DSS control, R-Y FMT, B-I FMT, and B-II FMT mice following 2.5% DSS or H_2O treatment; n = 6. (D) Differences in the whole colon in each group. (E) Total colon length in mice in each group; n = 6. (F) Spleen weight in mice in each group; n = 6. (G) H&E staining and Alcian blue staining in each group. (H) Histological scores (based on the assessment of intestinal mucosa and submucosal glandular structure disorder, distortion and the absence of crypt structures, the degree of immune cell infiltration, and affected area); n = 6. (I) Kaplan–Meier survival analysis of DSS control and R-Y FMT mice treated with 3.5% DSS; n = 10. Scale bars = 50 μm. Error bars represent the mean ± SEM. *$P < 0.05$, **$P < 0.01$, ***$P < 0.001$.

R-Y reconstruction reverses disordered gut microbiota and enriches SCFA-producing bacteria abundance

Compared to the B-I and B-II FMT groups, mice with R-Y FMT showed decreased inflammation levels and the inhibition of M1 macrophage polarization in colon tissues. Since previous studies reported the function of gut microbiota and its metabolites during

FMT, we also explored the underlying mechanisms of the effect by assessing alterations in microbiota and SCFA secretion in R-Y FMT mice.[29,36] Compared to the controls, the R-Y FMT model showed significantly elevated SCFA content in the colon, especially that of butyrate ($P < 0.01$, Fig. 5A and B). This suggests that R-Y FMT may promote the secretion of SCFAs.
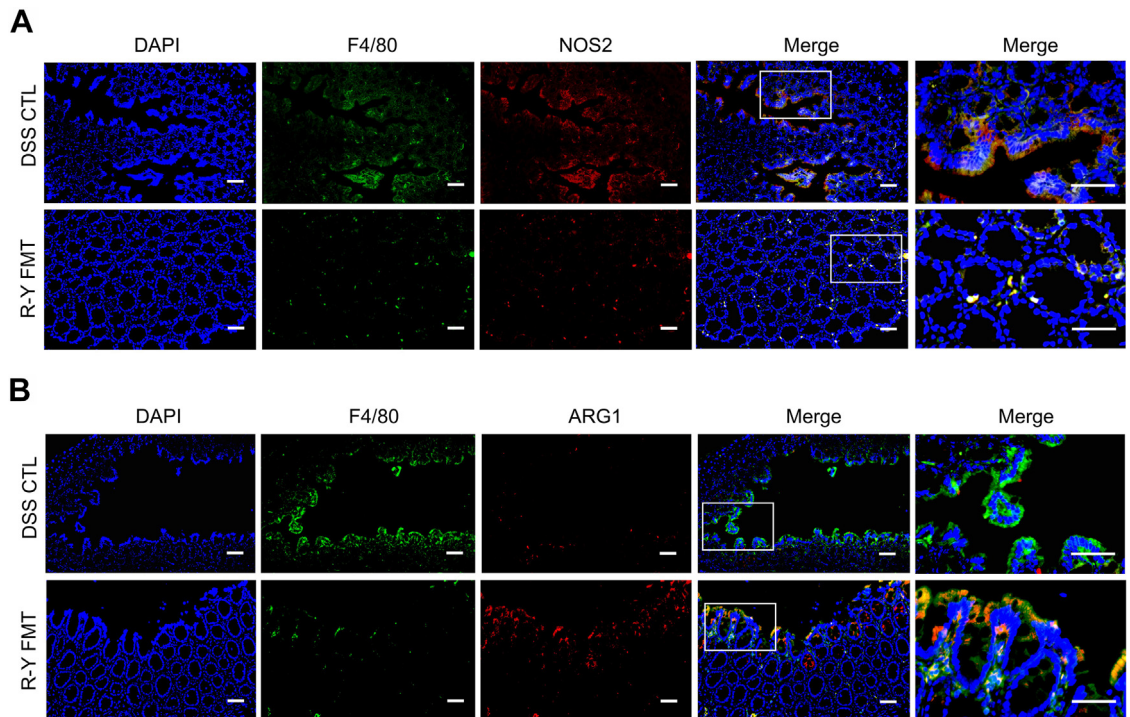
Fig. 4: F4/80$^+$NOS2$^+$ macrophages were decreased in R-Y FMT mice with DSS-treated colons. Representative images of immunofluorescence staining for (A) macrophage marker, F4/80 (green); M1 marker, NOS2 (red); and F4/80$^+$NOS2$^+$ cells (yellow, merge). (B) Macrophage marker, F4/80 (green); M2 marker, ARG1 (red); and F4/80$^+$ARG1$^+$ cells (yellow, merge). Cell nuclei, DAPI (blue). Representative merged images of at least three per group. Scale bars = 100 μm.

After confirming that the benefits of R-Y FMT were associated with SCFA secretion, we further determined the overall alteration in gut microbiota caused by R-Y reconstruction by analyzing the 16S-rRNA gene sequences of microbial samples collected from the feces of mice in the R-Y FMT and DSS control groups. According to the sequencing analysis, the Shannon and Simpson index values of patients in the R-Y group were significantly higher than those in the DSS control group ($P < 0.01$, $P < 0.01$, Fig. 5C and D). Bray–Curtis distance-based PCoA showed different clustering of gut microbiota communities between the R-Y FMT and DSS control groups (Fig. 5E). Then, we further performed a LEfSe analysis to evaluate effect size estimation, test biological consistency, and class comparison (Supplementary Figure S3). Compared to the control group, the relative abundance of *Bifidobacterium*, *Clostridium* and *Ruminococcus* were significantly enriched in the R-Y FMT group ($P < 0.01$, Fig. 5F). Moreover, these organisms were closely associated with the secretion of SCFAs.[27,31,32] Hence, the microbiota increased in abundance and played an anti-inflammatory role by secreting SCFAs to promote nutrient absorption in mice.

We also investigated the effects of SCFAs on M1 macrophage polarization *in vitro* in the RAW264.7 macrophage cell line treated with acetate, propionate, and butyrate (1 mM) for 8 h (Fig. 5G, Supplementary Figure S4A). The results revealed that the macrophage M1 polarization in the acetate, propionate and butyrate-treated groups was moderately lower than that in the control group. To further explore the effect of SCFAs on the pro-inflammatory process of macrophages, LPS was used to induce RAW264.7 M1 polarization. RAW264.7 cells were treated with different SCFAs (1 mM) along with LPS (100 ng/mL for 8 h) stimulation. The results indicated that SCFAs, especially butyrate, significantly inhibited the M1 polarization of macrophages (Fig. 5H, Supplementary Figure S4B).

### Butyrate restricts inflammation to improve nutrition absorption

Previous results indicated that butyrate secretion in R-Y FMT mice was greatly increased, and butyrate inhibited macrophage M1 polarization *in vitro*. To further confirm the effect of butyrate on colon inflammation *in vivo*, butyrate was added to the drinking water. In the *in vivo* experiments, butyrate treatment delayed reductions in weight compared to the DSS controls ($P < 0.05$, Fig. 6A). Intestinal inflammatory activity was also assessed by
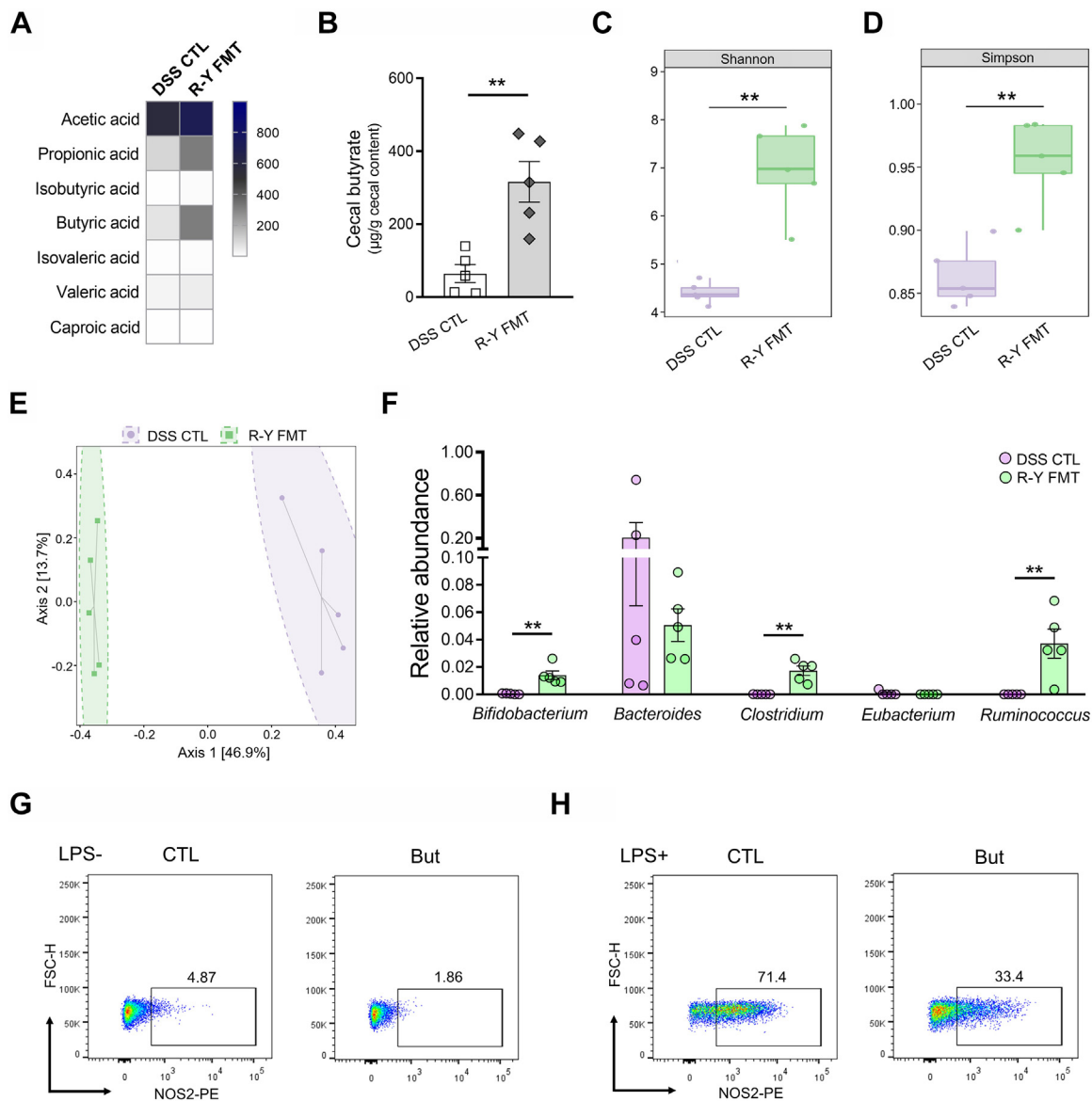
Fig. 5: The benefits of R-Y FMT were correlated with gut microbiota. (A) Heatmap of fecal SCFA concentrations; n = 5. (B) Differences in fecal butyrate concentrations between the DSS control and R-Y FMT mice; n = 5. (C and D) 16S-rRNA sequencing analysis of fecal samples from DSS control and R-Y FMT mice. Shannon and Simpson index analysis in each group. (E) PCoA plot from the DSS control and R-Y FMT mice groups based on the Bray–Curtis distance; n = 5. (F) Relative abundance of SCFA-producing microbes in mice feces; n = 5. (G) M1 macrophage polarization in the RAW264.7 macrophage cell line after butyrate treatment for 8 h. (H) Cells were treated with butyrate and LPS for 8 h to evaluate M1 macrophage polarization. Scale bars = 100 μm. The results are expressed as the mean ± SEM. $**P < 0.01$.

stool consistency, gross rectal bleeding, colon length, and spleen weight. Compared to the DSS control group, butyrate improved stool consistency and reversed gross rectal bleeding caused by DSS ($P < 0.05$, Fig. 6B and C). Although spleen weight was decreased by butyrate treatment ($P < 0.05$), colon lengths were not significantly different between the butyrate and control groups ($P > 0.05$, Fig. 6D–F). According to the results of H&E and Alcian blue staining and the histological score, butyrate eased intestinal inflammation to some extent, which may have contributed to the better nutrient levels in the mice in the butyrate group (Fig. 6G and H). Interestingly, although butyrate alleviated intestinal inflammation and reversed the trend toward weight loss caused by DSS, there was no significant difference in survival time between the butyrate-treated and control groups in mice treated with 3.5% DSS ($P > 0.05$, Fig. 6I).
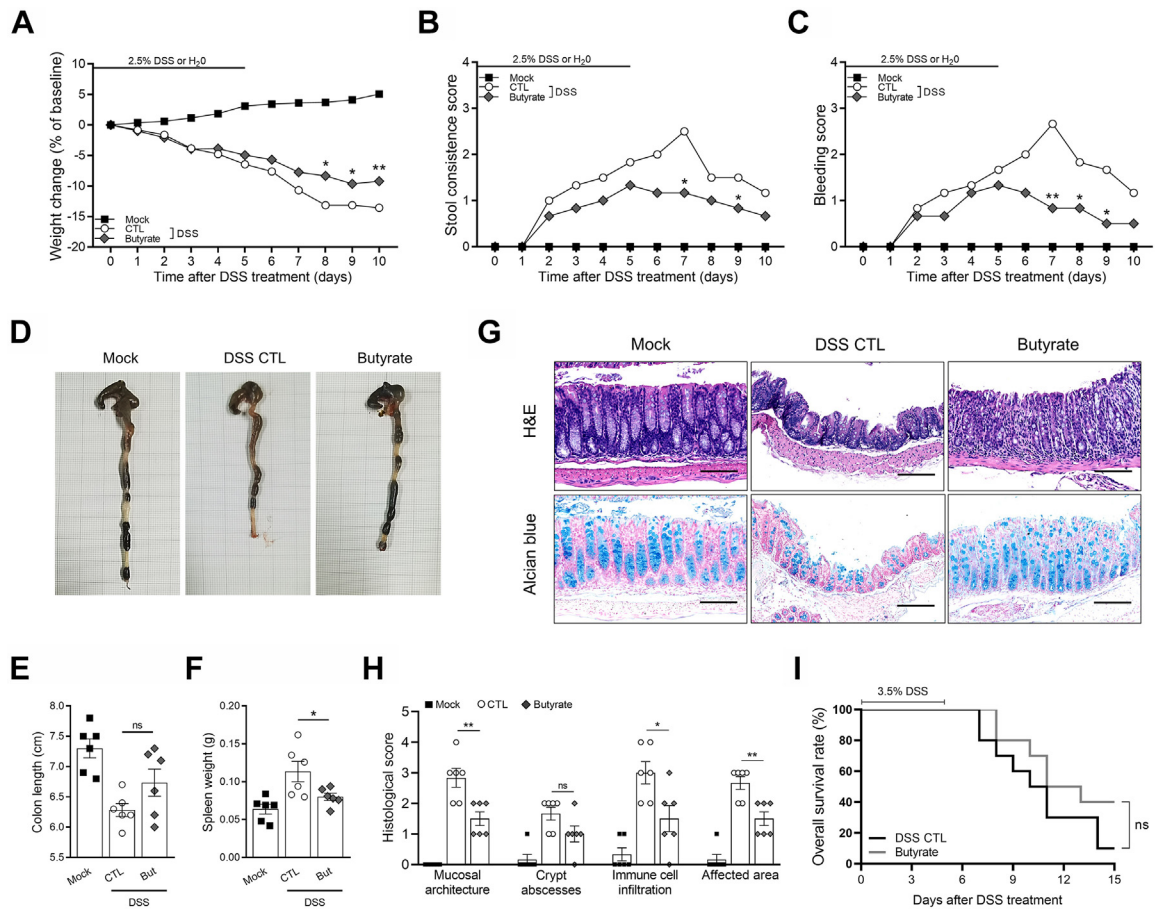
Fig. 6: Butyrate protects mice against colitis. (A–C) Mice in the butyrate group were given drinking water containing 2% butyrate. Weight change, stool consistency, and rectal bleeding scores in mock, DSS control, and butyrate mice following 2.5% DSS or H_2O treatment; n = 6. (D) Differences in the whole colon in each group. (E) Total colon length in the mice in each group; n = 6. (F) Spleen weight of mice in each group; n = 6. (G) H&E staining and Alcian blue staining. (H) Histological scores in each group; n = 6. (I) Kaplan–Meier survival analysis of DSS controls and butyrate-treated mice given 3.5% DSS; n = 10. Scale bars = 100 μm. Error bars represent the mean ± SEM. ns, no significance; *$P < 0.05$; **$P < 0.01$.

### R-Y FMT inhibits the NLRP3 signaling pathway by promoting butyrate secretion

The expression of NLRP3, an important regulatory target of the inflammatory pathway and pro-inflammatory mediators, was evaluated in the colons of mice treated with R-Y FMT or butyrate. The results showed a similar trend, that R-Y FMT or butyrate could efficiently block the activation of the NLRP3 inflammasome ($P < 0.05$, Fig. 7A–D). In addition, according to the mean density values, R-Y FMT and butyrate-treated mice showed the expression of caspase-1 and IL-1β, parameters of NLRP3 inflammasome activation, in colon tissues. We also found the same phenomena in mice colons using Western blotting. The NLRP3 expression level was obviously reduced in the colon tissues of R-Y FMT and the butyrate-treated DSS mouse model ($P < 0.01$, Fig. 7E and F). Down-regulation of the NLRP3 inflammasome was associated with butyrate secretion

promoted by bacterial transplantation from GC patients with R-Y reconstruction. We also detected the relative protein expression of caspase-1 and IL-1β in the colon tissues. Importantly, compared to the control group, the treatment groups showed lower levels of cleaved caspase-1 (P20) and mature IL-1β (P17) ($P < 0.05$, Fig. 7E and F).

Discussion

With the standardization and popularization of radical gastrectomy, B-I, B-II, and R-Y reconstructions have been widely used after distal gastrectomy. Comparative studies have confirmed that compared to B-I and B-II, R-Y reconstruction preserves the normal anatomical structure and can prevent bile reflux.[3] In patients with GC accompanied by type 2 diabetes mellitus, the clinical indicators of R-Y and B-II reconstruction were improved
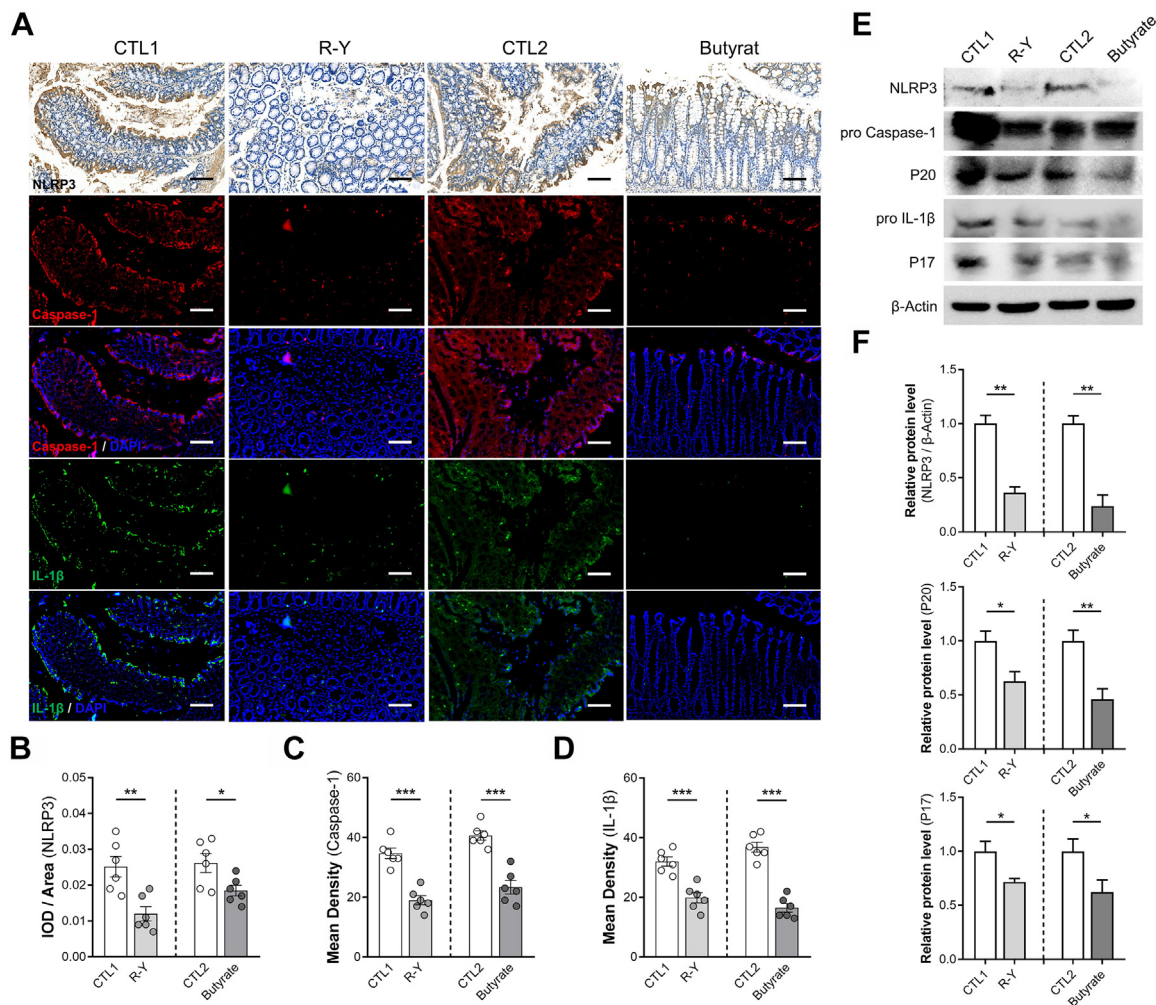
Fig. 7: R-Y FMT and butyrate inhibit NLRP3-associated pro-inflammatory mediator expression. (A) Representative immunohistochemical staining of NLRP3, and immunofluorescence staining of caspase-1 and IL-1β in colon specimens. (B) Quantification of NLRP3 expression using integrated optical density/specimen area (IOD/area); n = 6. (C and D) Quantification of caspase-1 and IL-1β in colon specimens using mean density (integrated density/specimen area); n = 6. (E) The expression levels of NLRP3, cleaved caspase-1 (P20), and mature IL-1β (P17) were detected in the colon tissues of R-Y FMT mice and the butyrate-treated mice colitis model. (F) The bands were quantified (n = 3). Scale bars = 100 μm. Error bars represent the mean ± SEM. *P < 0.05, **P < 0.01, ***P < 0.001.

by 27.8% and 5.9%, respectively, after radical gastrectomy, and the BMI was reduced accordingly.[9] These studies suggest that R-Y had better efficacy in alleviating morbid obesity and improving diabetes, especially for obese patients with a high BMI before surgery.

Although the purposes of bariatric and gastric cancer surgery are completely different, there are some anatomical and technical similarities between the two procedures. However, for partial GC patients with poor nutritional status before surgery, the influence of digestive tract reconstruction on postoperative nutritional status is uncertain, and the relevant mechanism is still unclear.[3,37,38] Interestingly, in our study, GC patients with poor basic nutritional status receiving R-Y

reconstruction after radical gastrectomy had a better BMI and SMI than patients who underwent B-I and B-II reconstructions. This finding is not completely consistent with those of studies on gastric constriction in obese patients or radical resection in GC patients.[37,39]

Recently, intestinal microbiota was linked to a variety of disease progressions.[40–43] We hypothesized that intestinal microbiota was involved in the improvement in postoperative nutritional status by R-Y reconstruction. With the advent of genomic sequencing and microbiota identification techniques, intestinal biodiversity has become increasingly clarified.[44,45] The intestinal microbiota has been shown to be closely related to the maintenance of health, and alterations in the microbiota

are associated with the development of many diseases. The main functions of the microbiota include regulating the host intestinal immune inflammatory responses, synthesizing a variety of biologically important small molecules and proteins, and regulating nutrient metabolism and absorption.[19] To explore the effect of intestinal microbiota changes in mice, we constructed a mouse intestinal inflammation model, and FMT was performed with feces collected from GC patients with B-I, B-II, and R-Y reconstructions one year after radical surgery. The results showed that the total colon length of the mice in the R-Y FMT group was longer and the spleen weight was lower than those in the other two groups. Moreover, the comprehensive structure of the intestinal glands was better, and macrophage infiltration was significantly reduced. F4/80+NOS2+ macrophages were also decreased in the colons of R-Y FMT mice treated with DSS, as shown by immunofluorescence staining. The findings suggest that the fecal bacteria in the R-Y group patients alleviated digestive tract inflammation in mice after transplantation. The 16S-rRNA sequencing analysis revealed that the relative abundance of SCFA-producing microbes in mice feces in the R-Y reconstruction group was significantly greater than that in the DSS control group. This finding may be closely related to the intestinal inflammation level.[46,47]

In patients with digestive tract reconstruction after radical gastrectomy, changes in the structure of the digestive tract, the abundance and proportion of intestinal microbiota, and its influence on fatty acid metabolism and further intestinal homeostasis is a complex biological process affected by multiple factors.[12,48] It is still unclear whether SCFAs, as important metabolites of intestinal microbiota, regulate immune cells in this process to reduce excessive immune responses caused by changes in colonic symbionts and maintain homeostasis in the internal environment. As a product of the anaerobic fermentation of dietary fiber, SCFAs are important substances that regulate intestinal immune responses.[19,49] Butyrate is thought to inhibit secondary reaction genes by recruiting the Mi-2/NuRD inhibitor complex, which allows Mi-2 to inhibit the chromatin remodeling of secondary reaction genes. Butyrate inhibits these pro-inflammatory mediators at the transcriptional level, resulting in the decreased recruitment of pol II and S5P to the NOS2, IL-6, and IL-12b promoters. These findings indicate the regulatory effect of butyrate on immunity.[50,51]

Changes in the structure of the digestive tract induce chronic intestinal inflammation, which is an important factor affecting intestinal nutrient absorption.[52–54] To clarify the regulation of butyrate on intestinal inflammation, and the relationship between intestinal inflammation caused by digestive tract reconstruction and nutrient absorption, we conducted relevant experiments *in vivo* and *in vitro*. We treated macrophages *in vitro* with both butyrate with LPS and the results suggested that

butyrate could effectively inhibit M1 macrophage polarization. Weight change, stool consistency, rectal bleeding scores, and histological scores were observed in the mock, DSS control, and butyrate groups in the *in vivo* experiments. The results indicated that butyrate could protect mice against colitis and promote nutrition absorption.

Previous studies indicated that the enhanced expression of butyrate could significantly decrease NLRP3 inflammasome formation and activation and block relevant inflammatory diseases.[27,28,55] The NLRP3 inflammasome is a multimeric cytosolic protein complex that promotes the maturation and release of IL-1β and IL-18 inflammatory cytokines, thus leading to the development of systemic inflammation.[13] After being activated, NLRP3 recruits the adaptor molecule apoptosis-associated speck-like protein containing a caspase recruitment domain (ASC), which, in turn, binds to pro-caspase-1, leading to autocatalytic processing and activation.[56] NLRP3 has been implicated in a wide range of diseases, including multiple myeloma, Alzheimer's disease, gout, type 2 diabetes, infectious diseases, systemic inflammation, cardiovascular mortality, and cancer.[56,57] The NLRP3 inflammasome also plays a critical role in regulating the balance of intestinal homeostasis and maintaining immune responses.[58]

Previous studies suggested that the deterioration of colitis was associated with enrichment in butyrate-producing bacteria and increased levels of cecal butyrate.[19] Evidence indicates that too much butyrate may harm the gut by inhibiting the proliferation of colonic epithelial stem.[59] Some studies reported that β-hydroxybutyrate rather than the structurally related SCFAs butyrate and acetate suppressed the activation of the NLRP3 inflammasome in intestinal inflammation.[55] In our study, the expression levels of NLRP3, cleaved caspase-1 (P20), and mature IL-1β (P17) were analyzed in the colon tissues of R-Y FMT mice and the butyrate-treated mice colitis model. The results showed that R-Y FMT inhibited NLRP3-associated pro-inflammatory mediator expression by promoting butyrate secretion. Butyrate may negatively regulate the inflammatory signaling pathway mediated by NLRP3 to inhibit the secretion of IL-1β and IL-18. The secretion of IL-1β and IL-18 is strictly regulated by the NLRP3 inflammasome. Upon NLRP3 inflammasome activation, active caspase-1 (P20) cleaves pro-IL-1β to produce the secretory mature IL-1β (P17).

Our study also had some limitations. Even though our analysis was data-driven, it requires further validation. Future prospective studies, including stricter inclusion and exclusion criteria, improved preoperative cohort demographics, detailed intestinal permeability and nutritional assessments, advanced and reliable methods such as the Bristol stool form, and perioperative glycolipid metabolism analysis, can demonstrate and support our hypothesis.[60–62] In addition, our study
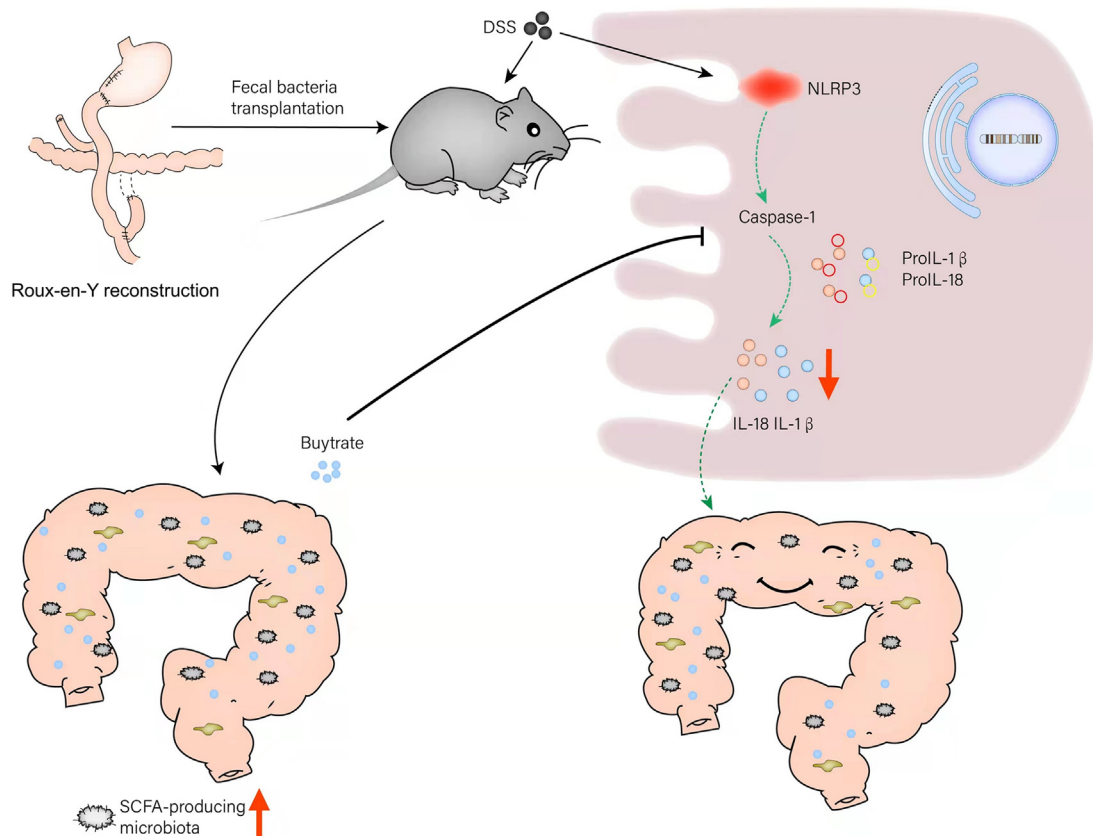
Fig. 8: Proposed model and the underlying mechanism by which gastrointestinal reconstruction after radical gastrectomy regulates the abundance of the gut microbiota to change the concentration of SCFAs, thereby affecting intestinal inflammation and nutrient absorption.

findings only apply to patients with distal gastrectomy, and whether this hypothesis is still applicable to patients with total gastrectomy or proximal gastrectomy remains to be further demonstrated. Meanwhile, we considered that the cohort could represent a wider population of interest to a certain degree. However, individual variation existed in this cohort, which would result in generalizability limitations. To further improve the representative capacity of the study cohort, we will expand it further, and repeat the analysis in other populations.

In summary, R-Y reconstruction alleviated intestinal inflammation by increasing the abundance of butyrate-producing bacteria and inhibiting the NLRP3 inflammasome by the butyrate produced, and ultimately, maintaining postoperative nutrient absorption in patients with poor basic nutrition (Fig. 8). Thus, R-Y reconstruction could be a qualified selection to regulate the gut microbiota to exert anti-inflammatory effects and produce the microbial metabolite butyrate for GC patients with poor basic nutritional status and has good clinical application potential.

Contributors
YY and SS conducted the acquisition, analysis, and interpretation of the data and drafting of the manuscript. YY, SS, JG, HN, KZ, QX, DZ, XW, and LG contributed to the analysis and interpretation of the data. JG, HN, KZ, and QX collected the samples. XZ designed the study, critically revised the manuscript and performed overall study supervision. YY, SS, and XZ verified the underlying data. All authors read and approved the final manuscript.

Data sharing statement
The raw reads of the microbiome data were deposited in the online repository available on the website. All other data and materials supporting the results or analyses presented in this paper are available upon reasonable request.

Appendix A. Supplementary data

Supplementary data related to this article can be found at https://doi.org/10.1016/j.ebiom.2022.104347.

References

1 Siegel RL, Miller KD, Jemal A. Cancer statistics, 2020. *CA Cancer J Clin*. 2020;70(1):7–30.
2 Feng RM, Zong YN, Cao SM, Xu RH. Current cancer situation in China: good or bad news from the 2018 Global Cancer Statistics? *Cancer Commun*. 2019;39(1):22.
3 So JB, Rao J, Wong AS, et al. Roux-en-Y or Billroth II reconstruction after radical distal gastrectomy for gastric cancer: a multicenter randomized controlled trial. *Ann Surg*. 2018;267(2):236–242.
4 Ruiz-Tovar J, Carbajo MA, Jimenez JM, et al. Long-term follow-up after sleeve gastrectomy versus Roux-en-Y gastric bypass versus one-anastomosis gastric bypass: a prospective randomized comparative study of weight loss and remission of comorbidities. *Surg Endosc*. 2019;33(2):401–410.
5 Okuno K, Nakagawa M, Kojima K, et al. Long-term functional outcomes of Roux-en-Y versus Billroth I reconstructions after laparoscopic distal gastrectomy for gastric cancer: a propensity-score matching analysis. *Surg Endosc*. 2018;32(11):4465–4471.
6 Virgilio E, Balducci G, Mercantini P, et al. Reconstruction after distal gastrectomy for gastric cancer: Billroth 2 or Roux-en-Y procedure? *Anticancer Res*. 2017;37(10):5595–5602.
7 Cuenca-Abente F, Puma R, Ithurralde-Argerich J, Faerberg A, Rosner L, Ferro D. Non-bariatric Roux-en-Y gastric bypass. *J Laparoendosc Adv Surg Tech*. 2020;30(1):31–35.
8 Nomura E, Kayano H, Lee SW, et al. Functional evaluations comparing the double-tract method and the jejunal interposition method following laparoscopic proximal gastrectomy for gastric cancer: an investigation including laparoscopic total gastrectomy. *Surg Today*. 2019;49(1):38–48.
9 Parmar CD, Bryant C, Luque-de-Leon E, et al. One anastomosis gastric bypass in morbidly obese patients with BMI >/= 50 kg/m(2): a systematic review comparing it with Roux-en-Y gastric bypass and sleeve gastrectomy. *Obes Surg*. 2019;29(9):3039–3046.
10 Lee TH, Lee CM, Park S, et al. Long-term follow-up for type 2 diabetes mellitus after gastrectomy in non-morbidly obese patients with gastric cancer: the legitimacy of onco-metabolic surgery. *J Gastric Cancer*. 2017;17(4):283–294.
11 Wang Y, Hooper LV. Immune control of the microbiota prevents obesity. *Science*. 2019;365(6451):316–317.
12 Costa M, Trovao Lima A, Morais T, et al. Does reconstruction type after gastric resection matters for type 2 diabetes improvement? *J Gastrointest Surg*. 2020;24(6):1269–1277.
13 Sharma BR, Kanneganti TD. NLRP3 inflammasome in cancer and metabolic diseases. *Nat Immunol*. 2021;22(5):550–559.
14 Sanchez-Lopez E, Zhong Z, Stubelius A, et al. Choline uptake and metabolism modulate macrophage IL-1beta and IL-18 production. *Cell Metab*. 2019;29(6):1350–1362. e7.
15 Lamkanfi M, Dixit VM. Mechanisms and functions of inflammasomes. *Cell*. 2014;157(5):1013–1022.
16 Wen H, Miao EA, Ting JP. Mechanisms of NOD-like receptor-associated inflammasome activation. *Immunity*. 2013;39(3):432–441.
17 Ratsimandresy RA, Dorfleutner A, Stehlik C. An update on PYRIN domain-containing pattern recognition receptors: from immunity to pathology. *Front Immunol*. 2013;4:440.
18 Chen Y, Pitzer AL, Li X, Li PL, Wang L, Zhang Y. Instigation of endothelial Nlrp3 inflammasome by adipokine visfatin promotes inter-endothelial junction disruption: role of HMGB1. *J Cell Mol Med*. 2015;19(12):2715–2727.
19 Singh V, Yeoh BS, Walker RE, et al. Microbiota fermentation-NLRP3 axis shapes the impact of dietary fibres on intestinal inflammation. *Gut*. 2019;68(10):1801–1812.
20 Xu C, Lu Z, Luo Y, et al. Targeting of NLRP3 inflammasome with gene editing for the amelioration of inflammatory diseases. *Nat Commun*. 2018;9(1):4092.
21 Jamsen E, Pajarinen J, Kouri VP, et al. Tumor necrosis factor primes and metal particles activate the NLRP3 inflammasome in human primary macrophages. *Acta Biomater*. 2020;108:347–357.
22 De Angelis I, Ricceri L, Vitale A. The 3R principle: 60 years taken well. Preface. *Ann Ist Super Sanita*. 2019;55(4):398–399.
23 Khalyfa A, Ericsson A, Qiao Z, Almendros I, Farre R, Gozal D. Circulating exosomes and gut microbiome induced insulin resistance in mice exposed to intermittent hypoxia: effects of physical activity. *EBioMedicine*. 2021;64:103208.
24 Charan J, Kantharia ND. How to calculate sample size in animal studies? *J Pharmacol Pharmacother*. 2013;4(1):303–306.
25 Yang S, He X, Zhao J, et al. Mitochondrial transcription factor A plays opposite roles in the initiation and progression of colitis-associated cancer. *Cancer Commun*. 2021;41(8):695–714.
26 Yao Y, Yang X, Sun L, et al. Fatty acid 2-hydroxylation inhibits tumor growth and increases sensitivity to cisplatin in gastric cancer. *EBioMedicine*. 2019;41:256–267.
27 Wu Y, He F, Zhang C, et al. Melatonin alleviates titanium nano-particles induced osteolysis via activation of butyrate/GPR109A signaling pathway. *J Nanobiotechnology*. 2021;19(1):170.
28 Shao X, Sun S, Zhou Y, et al. Bacteroides fragilis restricts colitis-associated cancer via negative regulation of the NLRP3 axis. *Cancer Lett*. 2021;523:170–181.
29 Li J, Zhao F, Wang Y, et al. Gut microbiota dysbiosis contributes to the development of hypertension. *Microbiome*. 2017;5(1):14.
30 Percie du Sert N, Hurst V, Ahluwalia A, et al. The ARRIVE guidelines 2.0: updated guidelines for reporting animal research. *PLoS Biol*. 2020;18(7):e3000410.
31 Yang B, Huang Z, He Z, et al. Protective effect of Bifidobacterium bifidum FSDJN7O5 and Bifidobacterium breve FHNFQ23M3 on diarrhea caused by enterotoxigenic Escherichia coli. *Food Funct*. 2021;12(16):7271–7282.
32 Zhu Z, Zhu L, Jiang L. Dynamic regulation of gut Clostridium-derived short-chain fatty acids. *Trends Biotechnol*. 2022;40(3):266–270.
33 Coletta R, Morabito A, Iyer K. Nontransplant surgery for intestinal failure. *Gastroenterol Clin North Am*. 2019;48(4):565–574.
34 Barbara G, Barbaro MR, Fuschi D, et al. Inflammatory and microbiota-related regulation of the intestinal epithelial barrier. *Front Nutr*. 2021;8:718356.
35 Zhuang H, Lv Q, Zhong C, et al. Tiliroside ameliorates ulcerative colitis by restoring the M1/M2 macrophage balance via the HIF-1alpha/glycolysis pathway. *Front Immunol*. 2021;12:649463.
36 Kong C, Yan X, Liu Y, et al. Ketogenic diet alleviates colitis by reduction of colonic group 3 innate lymphoid cells through altering gut microbiome. *Signal Transduct Target Ther*. 2021;6(1):154.
37 Tran TB, Worhunsky DJ, Squires MH, et al. To Roux or not to Roux: a comparison between Roux-en-Y and Billroth II reconstruction following partial gastrectomy for gastric cancer. *Gastric Cancer*. 2016;19(3):994–1001.
38 Gu L, Fu R, Chen P, et al. In terms of nutrition, the most suitable method for bariatric surgery: laparoscopic sleeve gastrectomy or Roux-en-Y gastric bypass? A systematic review and meta-analysis. *Obes Surg*. 2020;30(5):2003–2014.
39 Nakamura M, Nakamori M, Ojima T, et al. Randomized clinical trial comparing long-term quality of life for Billroth I versus Roux-en-Y reconstruction after distal gastrectomy for gastric cancer. *Br J Surg*. 2016;103(4):337–347.
40 Terrisse S, Derosa L, Iebba V, et al. Intestinal microbiota influences clinical outcome and side effects of early breast cancer treatment. *Cell Death Differ*. 2021;28(9):2778–2796.
41 Dong X, Pan P, Zheng DW, Bao P, Zeng X, Zhang XZ. Bio-inorganic hybrid bacteriophage for modulation of intestinal microbiota to remodel tumor-immune microenvironment against colorectal cancer. *Sci Adv*. 2020;6(20):eaba1590.
42 Yang J, Kim CJ, Go YS, et al. Intestinal microbiota control acute kidney injury severity by immune modulation. *Kidney Int*. 2020;98(4):932–946.
43 Wang J, Li F, Sun R, et al. Bacterial colonization dampens influenza-mediated acute lung injury via induction of M2 alveolar macrophages. *Nat Commun*. 2013;4:2106.
44 Kim H, Kim S, Jung S. Instruction of microbiome taxonomic profiling based on 16S rRNA sequencing. *J Microbiol*. 2020;58(3):193–205.
45 Johnson JS, Spakowicz DJ, Hong BY, et al. Evaluation of 16S rRNA gene sequencing for species and strain-level microbiome analysis. *Nat Commun*. 2019;10(1):5029.

46   Rogler G, Zaugg M. Nutrition-or lack Thereof-as a source of gut inflammation: evidence from basic science and clinical studies. *Mol Nutr Food Res.* 2021;65(5):e2001086.

47   Watson AJ. Effect of neonatal nutrition on long-term barrier function and gut inflammation. *Gastroenterology.* 2011;141(5):1939–1941.

48   Li HZ, Li N, Wang JJ, et al. Dysbiosis of gut microbiome affecting small intestine morphology and immune balance: a rhesus macaque model. *Zool Res.* 2020;41(1):20–31.

49   Schulthess J, Pandey S, Capitani M, et al. The short chain fatty acid butyrate imprints an antimicrobial program in macrophages. *Immunity.* 2019;50(2):432–445.e7.

50   Chang PV, Hao L, Offermanns S, Medzhitov R. The microbial metabolite butyrate regulates intestinal macrophage function via histone deacetylase inhibition. *Proc Natl Acad Sci U S A.* 2014;111(6):2247–2252.

51   Tye H, Yu CH, Simms LA, et al. NLRP1 restricts butyrate producing commensals to exacerbate inflammatory bowel disease. *Nat Commun.* 2018;9(1):3728.

52   Lalles JP. Recent advances in intestinal alkaline phosphatase, inflammation, and nutrition. *Nutr Rev.* 2019;77(10):710–724.

53   Weingarden AR, Vaughn BP. Intestinal microbiota, fecal microbiota transplantation, and inflammatory bowel disease. *Gut Microb.* 2017;8(3):238–252.

54   Farre R, Fiorani M, Abdu Rahiman S, Matteoli G. Intestinal permeability, inflammation and the role of nutrients. *Nutrients.* 2020;12(4):1185.

55   Yuan X, Wang L, Bhat OM, Lohner H, Li PL. Differential effects of short chain fatty acids on endothelial Nlrp3 inflammasome activation and neointima formation: antioxidant action of butyrate. *Redox Biol.* 2018;16:21–31.

56   Hofbauer D, Mougiakakos D, Broggini L, et al. beta2-microglobulin triggers NLRP3 inflammasome activation in tumor-associated macrophages to promote multiple myeloma progression. *Immunity.* 2021;54(8):1772–1787.e9.

57   Schunk SJ, Kleber ME, Marz W, et al. Genetically determined NLRP3 inflammasome activation associates with systemic inflammation and cardiovascular mortality. *Eur Heart J.* 2021;42(18):1742–1756.

58   Zaki MH, Lamkanfi M, Kanneganti TD. The Nlrp3 inflammasome: contributions to intestinal homeostasis. *Trends Immunol.* 2011;32(4):171–179.

59   Kaiko GE, Ryu SH, Koues OI, et al. The colonic crypt protects stem cells from microbiota-derived metabolites. *Cell.* 2016;165(7):1708–1720.

60   Vork L, Wilms E, Penders J, Jonkers D. Stool consistency: looking beyond the Bristol stool form scale. *J Neurogastroenterol Motil.* 2019;25(4):625.

61   Blake MR, Raker JM, Whelan K. Validity and reliability of the Bristol stool form scale in healthy adults and patients with diarrhoea-predominant irritable bowel syndrome. *Aliment Pharmacol Ther.* 2016;44(7):693–703.

62   Shuai M, Zuo LS, Miao Z, et al. Multi-omics analyses reveal relationships among dairy consumption, gut microbiota and cardiometabolic health. *EBioMedicine.* 2021;66:103284.